# JOURNAL OF TECHNIQUES

Journal homepage*: http://journal.mtu.edu.iq*

# High Impedance Fault Detection in Distribution Feeder Based on Spectrum Analysis and ANN with Non-Linear Load

Mohammed Naisan Allawi[1*], Ali Nasser Hussain[1], Mousa K. Wali[1], Daniel Augusto Pereira[2]

[1]Electrical Engineering Technical College, Middle Technical University, Baghdad, Iraq

[2]Universidade Federal de Lavras, Lavras, Brazil

* Corresponding author E-mail: mohammednaissan@yahoo.com

| Article Info. | Abstract |
|---|---|
| | High Impedance Fault (HIF) detection in distribution networks is challenging for protection engineers, mainly because HIFs possess unique characteristics, including non-linearity, asymmetry, randomness, and relatively low fault current levels compared to the feeder load current. In this regard, the study proposes an approach to detect HIFs in a radial distribution feeder based on the spectrum analysis of current signals at the substation bus. The proposed method comprises two stages: signal decomposition and feature extraction. Fast Fourier Transform (FFT) is utilized for signal decomposition, followed by feature extraction. These features are subsequently used as input to an artificial neural network (ANN) to distinguish HIF from non-HIF events, such as linear and non-linear load switching, capacitor bank switching, and transformer energization. The proposed method's efficacy is rigorously evaluated under various dynamic conditions, demonstrating that the method can detect and differentiate HIFs from non-fault events with a high detection rate and high accuracy of 99.3%, irrespective of the HIF location and fault resistance. |

## 1. Introduction

High impedance fault (HIF) is a prevalent concern in power distribution networks. The Working Group on HIF Detection technique, operating under the purview of the IEEE Power System Relay Committee, defines HIFs as faults that produce inadequate fault current to be detected by conventional overcurrent protective devices, such as relays or fuses[1, 2]. These faults occur when a power line comes into contact with high-resistive surfaces such as asphalt, grass, sand, and tree branches or when a line breaks and touches the nonzero-resistance surfaces, resulting in a significant hazard to people and public safety[3-5]. This fault, usually accompanied by an electric arc, causes massive fires, leading to costly damages and potential loss of life. Despite the severity of HIFs, diagnosing these faults remains challenging due to their peculiar characteristics and low current draw, typically less than 75 A [5, 6]. According to Electrical safety reports, only 17.5% of HIFs were detected and eliminated by traditional protection techniques such as over-current relays. As a result, identifying HIFs remains a significant obstacle in the power distribution field, requiring effective solutions to ensure public safety and minimize damages [7, 8].

## 2. Literature Review

The researchers discussed various techniques in the literature to detect HIF in distribution systems. Methods for detecting high-impedance faults are often classified as either mechanical or electrical. The mechanical technique forces the line to contact the ground when it is broken or falls to a high resistive surface to activate the overcurrent protection relay [9]. However, these solutions have been found to be relatively costly and unreliable in their performance. In contrast, electrical methods employ traditional techniques for HIF detection, such as monitoring the zero-sequence current, which is used as an indicator of ground faults. These techniques can be unreliable because loads are usually unbalanced, and the zero-sequence current is always present. Consequently, the relay must be set to a specific tolerance level to prevent false trips, making it more challenging to identify HIFs [5]. Other methods utilize various signal processing-based techniques for HIF detection. These techniques are classified based on domain analysis into the time, frequency, time scale, and time-frequency domains [6, 10]. Time-domain methods that employ behavior analysis, magnitudes, and sequences as detecting factors have been presented as an alternative to conventional mechanical procedures. These procedures are economical and have a fast response. However, it is vulnerable and inefficient to differentiate HIF from similar events in distribution systems, such as switching events, inrush current due to transformer energizing, and capacitor bank switching [11]. Some ways to extract temporal irregularities from HIF waveforms in the time domain include the active power dissipation factor, the sequence components of three-phase currents, and the amplitude, RMS, peak, and mean values. These techniques are insufficient to

| Nomenclature & Symbols | | | |
|---|---|---|---|
| ANN | Artificial Neural Network | IRC | Inrush Current due to Transformer Energization |
| CBS | Capacitor Bank Switching | LS | Load Switching |
| EPDF | Electrical Power Distribution Feeder | NLL | Non-Linear Load |
| F | Frequency | P | Power |
| FFT | Fast Fourier Transform | PSD | Power Spectrum Density |
| FN | False Negative | TN | True Negative |
| FP | False Positive | TP | True Positive |
| FS | Frequency Spectrum | $h_i$ | Harmonic magnitude at i order |
| HIF | High impedance fault | Vph | Phase Voltage |
| HLNN | Hidden Layer Neural Network | | |

describe the irregularity of HIF, and their detection requires more intricate time-domain calculations. The authors also proposed mathematical morphological techniques in the time domain to identify HIF [6, 11]. The Fast Fourier transform-based technique was used for signal analysis in the frequency domain. In reference [11], the authors utilized FFT to extract even and odd harmonics, effectively detecting High Impedance Faults (HIF) and distinguishing them from other events occurring in the distribution system. Moreover, the authors in reference [3] utilized the even-harmonic in the voltage waveform as a feature to detect HIF in the distribution system. Wavelet transform is used for current signal analysis to extract the appropriate features in the time scale domain. The Maximal Overlap Discrete Wavelet Packet Transform (MODWPT) and a specific knot-based Empirical Mode Decomposition (EMD) algorithm are used by [10] to separate inter harmonic of the current signal and use it as a feature to detect HIF. The authors in [12] proposed Discrete Wavelet Transform (DWT) for signal processing and feature extraction, and then used Decision Tree (DT) as a feature classifier to identify HIF from other non-HIF events. Empirical Wavelet transform and Support Vector Machine (SVM) are presented by [13] for feature extraction and classification, respectively, to differentiate HIF from switching events in the distribution system. The DWT is utilized in [14] to extract the features, and feature classification is accomplished using an evolving neural network (ENN). Time-frequency-based approaches such as Short Time Fourier Transform (STFT), Stockwell Transform (ST), and Hermite Transform (HT) are regarded as effective methods for nonstationary signal analysis. STFT is used as a feature extraction technique in [15], and a Convolutional Neural Network (CNN) as a feature classifier. ST is utilized in [16] to extract the third harmonic current phase angle. Continuous monitoring of this feature is carried out with a moving standard deviation as an indicator to identify HIF. In reference [17], Hermite Transform (HT) was utilized to extract relevant features and then used K-Nearest Neighbor (KNN) to classify and differentiate HIF from other healthy events. A modified Gabor Wigner Transform (WT) was used in [8] to extract features in the form of 2-D scalograms, and a CNN was utilized for HIF identification and classification. Empirical Mode Decomposition (EMD) and Artificial Neural Networks (ANN) were proposed in [18, 19] to identify HIF. This approach uses the harmonic content of the current signal for feature classification.

In this context, increasing the non-linear loads, such as TV and other loads with an electronic device in the power distribution grid, makes detecting HIF challenging. This is because the transient states of non-linear loads exhibit behaviors similar to those of HIFs, making it difficult to differentiate between them. Many previous studies have neglected to consider this when building HIF detection techniques, resulting in reduced detection reliability. Furthermore, some research has also neglected to consider the presence of inrush currents caused by transformer saturation and heavy load switching in test scenarios. In this paper, an approach is proposed for the detection of high impedance faults (HIF) in distribution feeders. The method involves analyzing the Frequency Spectrum (FS) and Power Spectral Density (PSD) of the current signal during HIF and other events to extract the relevant features, which are subsequently fed into an ANN to differentiate HIF from non-HIF events. The proposed method has been rigorously evaluated under various dynamic conditions, including non-linear load, for various test scenarios. The rest of this paper is structured as follows. Section 3 will detail the test system. Following this, in Section 4, the proposed methodology of this study. The results and discussions are presented in section 5. Finally, the conclusions are illustrated in Section 6.

## 3. The Test System

Acquiring fault information from the electrical power distribution feeder (EPDF) is challenging for technical and economic reasons. Consequently, a model of (EPDF) has been developed using MATLAB/SIMULINK in this research to simulate HIF and other non-HIF events.

### 3.1. System modeling

A MATLAB/Simulink model has been developed to represent a radial overhead electrical power distribution feeder (EPDF), as shown in Fig. 1. The feeder comprises a 33kV/50Hz grid source, a 10MVA substation transformer with a voltage ratio of 33/11kV, and two three-phase line sections with a length of 5km each. The system is designed to handle a rated load of 5MVA with a power factor of 0.85. To simulate common loading scenarios, the (EPDF) model contains both linear and non-linear loads. An AC/DC converter is modeled in this study as the non-linear load, as illustrated in Fig. 2. A three-phase capacitor bank has been installed at the substation busbar to improve the power factor from 0.85 to 0.95.

### 3.2. HIF model and characteristics

Typically, HIF involves an electric arc, which provides fault currents with peculiar characteristics such as:

- Asymmetry: the peak values of the fault currents are different for the positive and negative halves of the cycle.
- Non-linearity: the characteristic curve of voltage and current is non-linear.
- Buildup: the size of the current progressively grows until it reaches its maximum value.
- Randomness: the instability of the fault circuit, induced by the oscillation of the tree branch, results in the fault current displaying stochastic characteristics [6, 20].

To emulate these characteristics, researchers developed various HIF models. The HIF model, depicted in Fig. 3, was used in this study and is based on Emanuel's model [10]. It consists of two variable resistances ($R_p$ , $R_n$) connected in series with antiparallel diodes ($D_p$ , $D_n$) and two variable dc sources ($V_p$ , $V_n$). The DC sources have varying magnitudes, representing the voltage between the high-impedance surface and the

power line. The current flows to the ground and then backward, dependent on the value of the phasephase voltage of the power line $V_{ph}$ and the dc voltage sources; however, there is no flow of current when ($V_p \leq V_{ph} \leq V_n$), which represents the arc extinction time [21]. The proposed simulation model can simulate HIF with a greater degree of accuracy under a variety of high-resistive surfaces. Fig. 4a depicts the recorded current and voltage waveform at the HIF point, and Fig. 4b shows the relationship between the voltage and current at the fault point. According to the HIF model under consideration, the current waveform exhibits non-linearity, asymmetry, and randomness. In this study, the parameters of the HIF model for five different surfaces are utilized, as illustrated in Table 1. The values of the resistances and DC voltage sources vary in a specific ratio, with a variation time of 0.1 MS, to simulate the random phenomena associated with HIF [2, 22].

*3.3. Test scenario*

As demonstrated in the simulation scenarios presented in Table 2, various events, including HIF events, linear and non-linear load switching, capacitor bank switching, and inrush current due to transformer saturation, were all simulated. The complete data set for this test comprises one thousand three hundred forty-four (1344) cases.
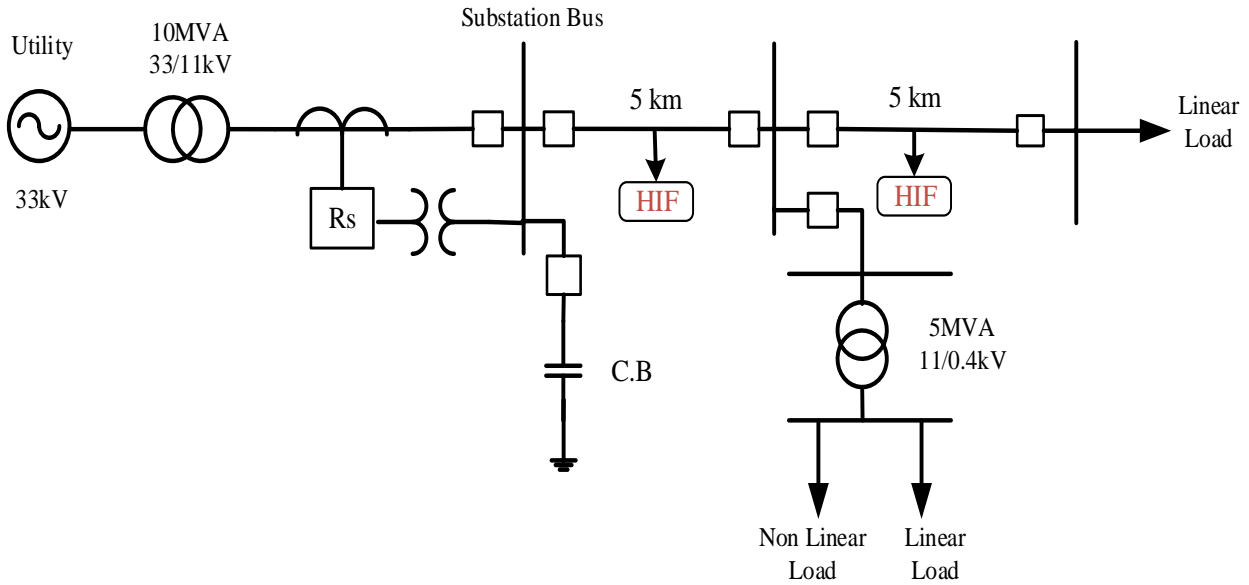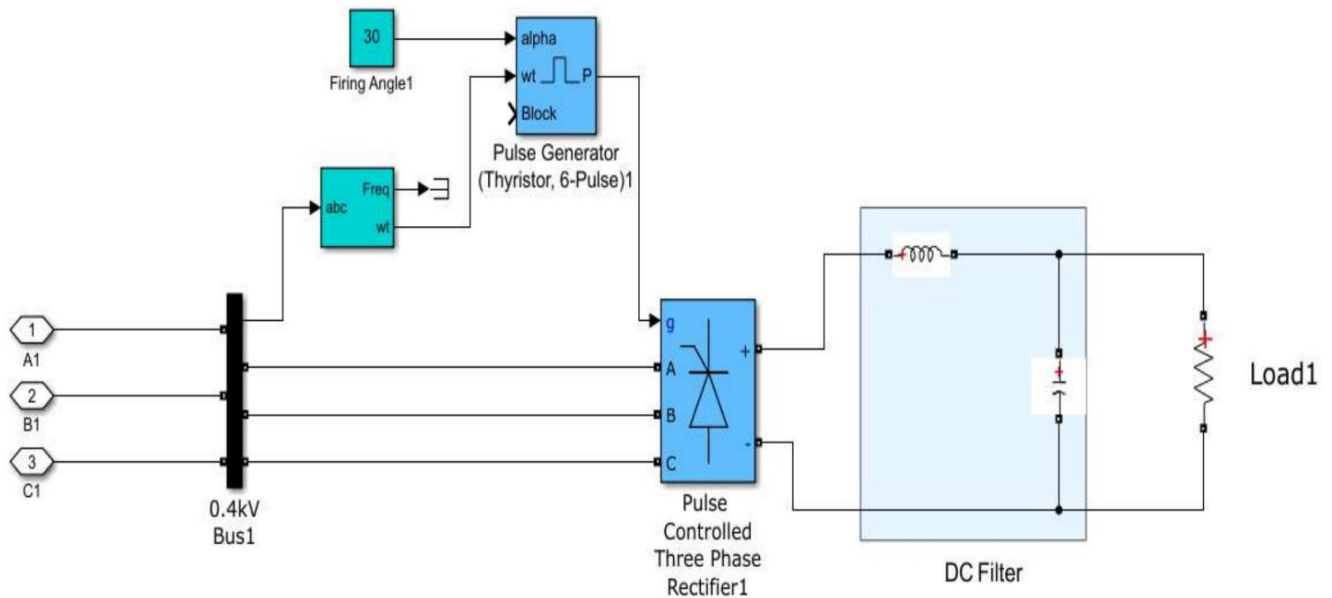


Fig. 1. Electrical power distribution feeder
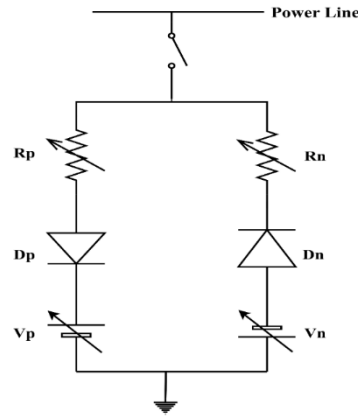


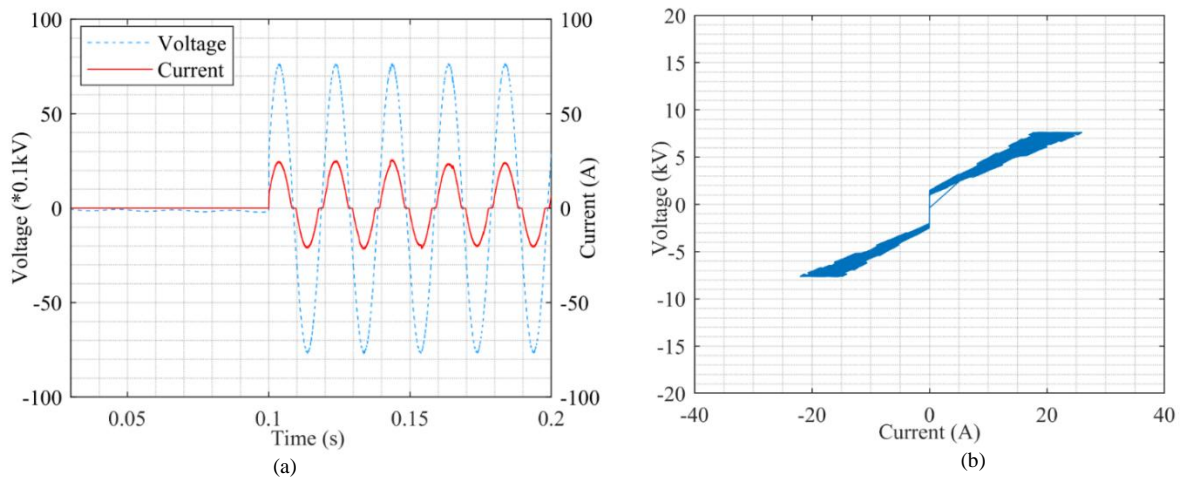Fig. 2. AC/DC Converter

Fig. 3. HIF model



(a)

(b)

Fig. 4. a) Voltage and current waveform at fault point, b) V-I Characteristics at fault point

Table 1. Parameters of the HIF Model

| Surfaces | $R_p$ (Ω) | $R_n$ (Ω) | $V_p$ (V) | $V_n$ (V) |
|----------|-----------|-----------|-----------|-----------|
| 1 | 400±10% | 400±10% | 1250±150 | 2250±150 |
| 2 | 250±10% | 250±10% | 1100±250 | 2000±250 |
| 3 | 170±10% | 170±10% | 4800±350 | 5180±350 |
| 4 | 125±10% | 125±10% | 1400±300 | 2150±300 |
| 5 | 115±10% | 115±10% | 6100±500 | 6400±500 |

Table 2. Simulation Scenarios

| Events | Simulation Scenario | Total Scenarios |
|--------|--------------------|-----------------|
| HIF | Three Different Locations (2, 4.5, 9 km)<br>Five HIF Surfaces (Table 1)<br>Inception angle (0:30:330)<br>Loading Ratio (25%, 50%, 75%, 100%) | HIF (720) |
| LS | Loading Ratio (25%, 50%, 75%, 100%)<br>In Forward and Reverse Condition<br>Inception angle (0:30:330) | |
| CBS | On and Off Switching State<br>Inception angle (0:30:330)<br>Loading Ratio (25%, 50%, 75%, 100%) | Non-HIF (624) |
| IRC | Three Transformer Rating (0.5, 1, 1.5) MVA<br>Inception angle (0:30:330)<br>Loading Ratio (25%, 50%, 75%, 100%) | |
| NLL | NLL Percentage (0.25,0.35,0.55,0.7,0.85,1)<br>Inception angle (0:30:330)<br>Loading Ratio (25%,50%,75%,100%) | |

**4. The Proposed Methodology**

This paper presents the detection of HIF in a distribution feeder using the FS and PSD magnitude and uses ANN as an intelligent classifier. Fig. 5 depicts the steps of the process and is explained below:

*4.1. Data acquisition*

In this case, the distributed feeder was simulated in MATLAB/Simulink, the features of the current signal at the substation bus are recorded using FFT Analyzer under different conditions, as shown in the test scenario for HIF, and Non-fault events, such as capacitor bank switching, linear and non-linear load switching, and inrush current due to transformer energization.

*4.2. Feature extraction*

During this step, FFT is used to decompose the current signal in the frequency domain under faulty and non-faulty situations. Then the PSD and FS are calculated for different conditions. The features that are used are illustrated below:

F1 represents the value of the divide $3^{rd}$ and $2^{nd}$ Harmonic magnitude.

- F2 represents the average magnitude of odd harmonics and is calculated using Eq. 1.

$$F2 = \frac{1}{N}\sum_{i=1}^{N} h_{2i+1} \qquad N = 5 \tag{1}$$

- F3 represents the average magnitude of even harmonics and is calculated using Eq. 2.

$$F3 = \frac{1}{N}\sum_{i=1}^{N} h_{2i} \qquad N = 4 \tag{2}$$

- F4 represents the average of the divide odd harmonic (3/5, 3/7, 7/9, 9/11).
- F5 represents the inter harmonic energy.
- F6 represents the power spectrum density (PSD).

*4.3. Training and predicted step*

The extracted features under different simulation conditions in the scenario test are used to train the ANN. The total dataset consists of 1344 data samples, with 720 data samples for HIF and 624 for non-fault events generated from the simulated signals. It is randomly divided into 70% for training and 15% for testing and validation to identify HIF from other events in the distribution system. The output of NN is either 1 or 0, where 1 indicates HIF and 0 indicates HIF non-HIF events.
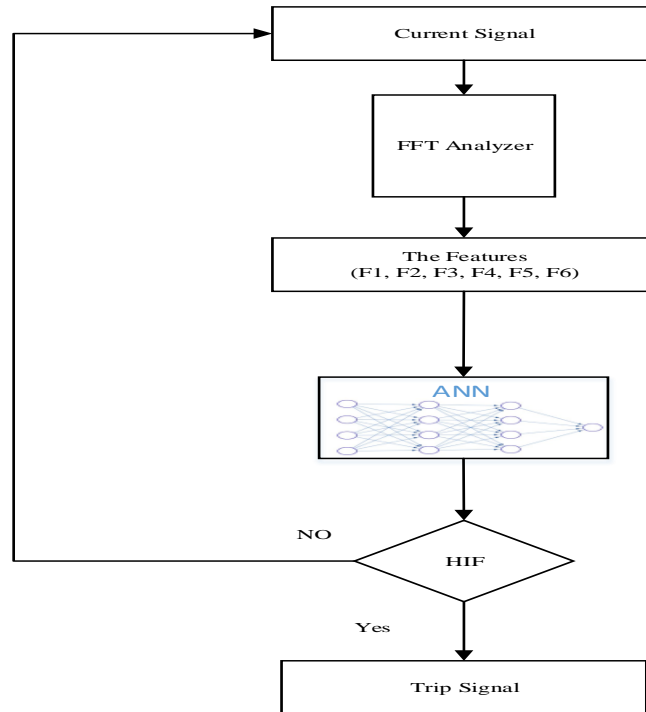


Fig. 5. Flowchart of the proposed methodology

*4.4. Signal processing technique*

In this study, the Discrete Fourier Transform (DFT) technique is employed as the signal decomposition method. The DFT transforms a time-domain signal into a frequency-domain representation, which can be utilized to extract significant features such as the FS and PSD. The Fast Fourier Transform (FFT) is adopted in this study as a rapid and efficient algorithm for computing the DFT coefficients. For a sampled signal x(n), the Fourier coefficient X(k) is determined using Eq. 3 as follows:

$$X(k) = \sum_{n=0}^{N-1} x(n)e^{-j\frac{2\pi kn}{N}} \quad , \qquad k = 0,1,2,3,\ldots,N-1 \tag{3}$$

Where x(n) is the samples of the signal in the time domain, N is the number of samples, and k is the frequency index.

The FS of a signal may be determined by calculating the magnitude of the FFT, which provides the magnitude of each frequency component present within the signal. Eq. 4, presented, illustrates the calculation of the FFT's magnitude:

$$|X(k)| = \sqrt{(Re(X(k)^2) + Im(X(k)^2))} \tag{4}$$

Where X(k) is the kth frequency component and Re(X(k)) and Im(X(k)) are the real and imaginary parts of X(k), respectively. The FFT is used to decompose a signal into its constituent harmonics, allowing for the identification of the frequencies and amplitudes of the harmonics present in the signal. This information is crucial for characterizing the signal [23-25]. PSD measures a signal's power content as a frequency function. It represents the power distribution across a signal's different frequency components [25], and the PSD is calculated as demonstrated in Eqs. 5 and 6.

$$PSD(k) = \frac{|X(k)|^2}{N} \tag{5}$$

To calculate the magnitude of PSD.

$$PSD = \sum_{k=0}^{N-1} PSD(k) \tag{6}$$

FS and PSD of the current signal during HIF and non-fault events, such as linear and non-linear load switching, capacitor bank switching, and transformer energization, are calculated using FFT. Data for these events are acquired using a 20 kHz sampling frequency to generate training and testing datasets. The events were applied at 0.1 s, and a five-cycle window was employed for signal processing to create data in both the presence and absence of HIF.

*4.5. Artificial Neural Networks (ANNs)*

ANNs are a potent programming tool for defect detection and classification that can address non-linear issues [26]. It has been demonstrated that ANN is an effective supervised learning method widely employed in machine learning [17]. A notable benefit of ANN is its capacity for parallel computation. This paper uses the Backpropagation Neural Network (BPNN) training algorithm to train the neural network (NN) and minimize errors between the desired and actual output. The back-propagation technique adjusts neuron weights in successive steps to reduce the difference between actual and desired outputs. An error signal is generated by subtracting the actual response of the network from the desired response. This erroneous signal is propagated against the direction of synaptic connections throughout the network, as shown in Fig. 6. Adjusting the weights brings the actual network response closer to the planned network response. In this study, the activation function chosen for both the hidden layers and output layers is the Sigmoid function [26, 27]. The NN training goal is set at a Mean Square Error (MSE) of 1%, and the Levenberg-Marquardt algorithm is employed as a fast method to update the weights and biases values. -
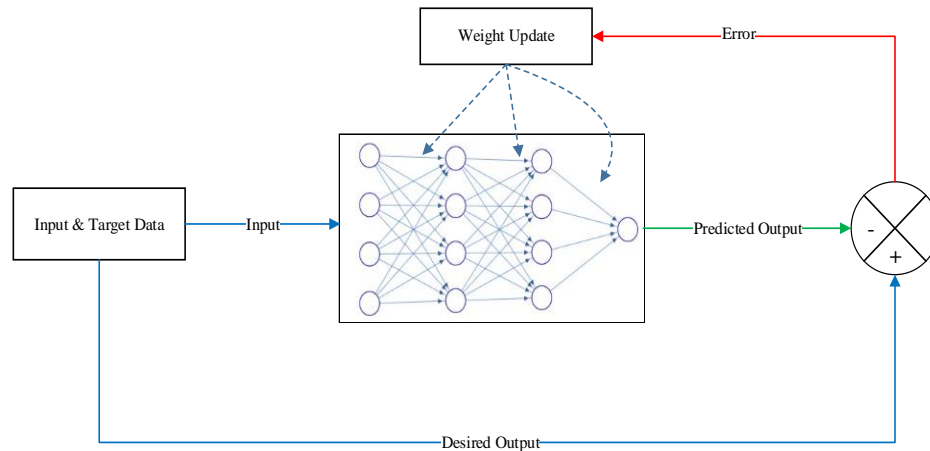


Fig. 6. The Process of the BPNN algorithm

*4.6. Performance metrics*

Various indices have been used to assess the effectiveness of intelligence classifiers such as Accuracy, Recall, Precision, and F1-score [8P3].

Accuracy is defined as the ratio of the number of correct predictions to the total number of predictions, as illustrated in Eq. 7.

$$\text{Accuracy} = \frac{TP + TN}{TP + TN + FP + FN} \tag{7}$$

Precision is the ratio of the true positives (TP) to the total number of positive predictions, as depicted in Eq. 8.

$$\text{Precision} = \frac{TP}{TP + FP} \tag{8}$$

Recall: It determines how many positive occurrences in the data the model correctly recognizes or how well it can avoid making incorrect negative predictions, as illustrated in Eq. 9.

$$\text{Recall} = \frac{TP}{TP + FN} \tag{9}$$

F1-score: The F1 score is a number between 0 and 1, with 1 representing the highest possible result. A high F1-score shows that the model can attain high precision and recall simultaneously, as shown in Eq. 10.

$$F1 - score = 2 \times \frac{\text{Recall} \times \text{Precision}}{\text{Recall} + \text{Precision}} \tag{10}$$

Mean Square Error (MSE) performance of the validation test, as illustrated in Eq. 11.

$$MSE = \frac{1}{N} \sum_{1}^{N} (y_{pred} - y_{targ})^2 \tag{11}$$

Where TP refers to the number of fault types that were correctly identified, while TN represents the number of non-fault cases that were accurately identified, on the other hand, FP indicates the number of fault types that were incorrectly identified, and FN represents the number of non-fault cases that were erroneously identified [28-31].

## 5. Result and Discussion

High impedance fault (HIF) detection is carried out on the distribution feeder, shown in Fig. 1. All simulations are performed using MATLAB/Simulink with a sampling frequency of 20 kHz. The dataset obtained from the simulation comprises both HIF and non-fault events, including linear and nonlinear load-switching events, capacitor bank switching, and transformer energization. The proposed method has been rigorously evaluated under various conditions, such as fault locations, inception angles, loading ratios, and different HIF surfaces, as demonstrated in the test scenarios. The FS and PSD of the current signal for HIF as well as other normal events are displayed in Fig. 7 (a-d) and Fig. 8.



(a)

(b)

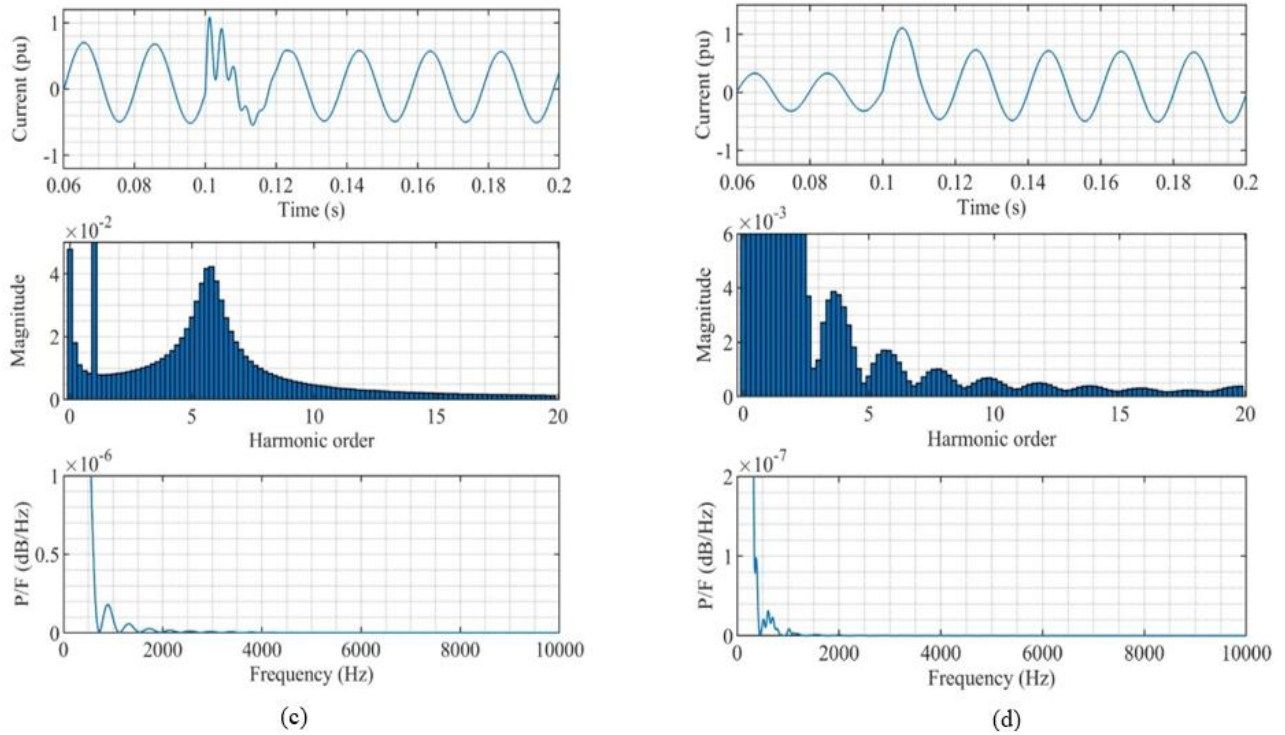(c)                                    (d)
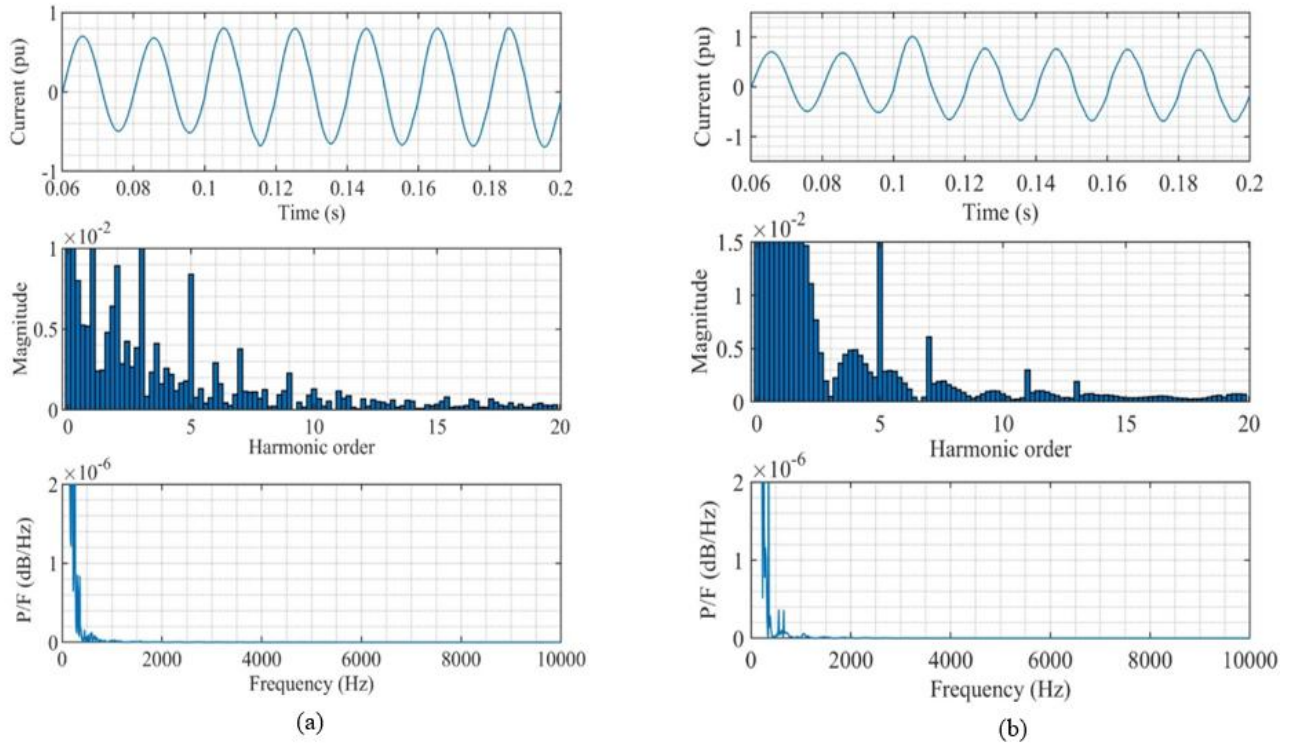
Fig. 7. The current signal at the substation bus, FS, and PSD for a) HIF event, b) NLL event, c) CBS event, d) LS event
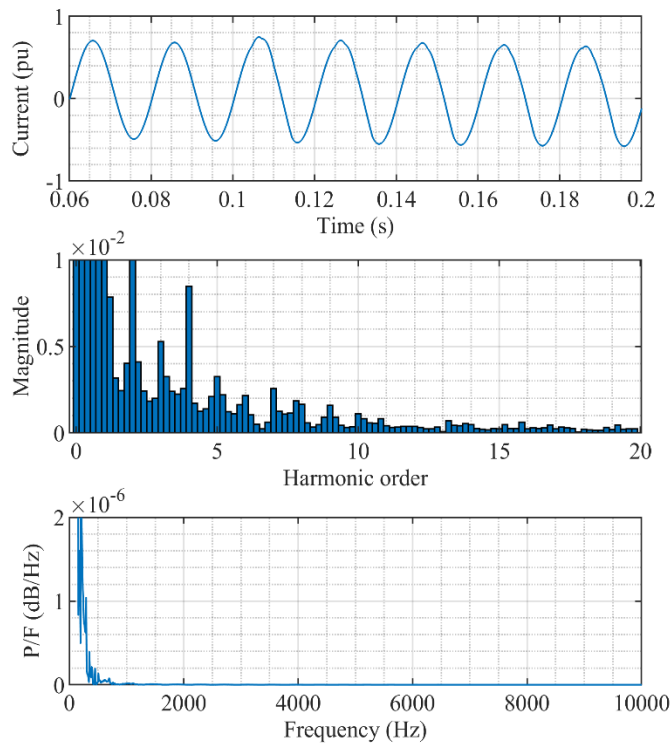


Fig. 8 The current signal at the substation bus, FS, and PSD for the INR event

In this study, the extracted features are categorized into six classes to examine the effect of each feature on overall classification performance, as illustrated in Table 3. It is important to note that the transient conditions that occur during switching events and transformer energization result in an increase in even harmonics, particularly second-order harmonics. Moreover, the HIF causes an increase in harmonics of odd order, specifically the third harmonic. Therefore, the relationship between the third and second harmonics (F1) can be utilized as a diagnostic feature to differentiate HIFs from natural occurrences [2]. However, this feature is not consistently reliable, particularly in non-linear loads, capacitor bank switching, and low and high-load switching cases. As depicted in Fig. 9, the detection performance is suboptimal. Specifically, the accuracy did not surpass 92.5% for different hidden layer neural network structures (HLNNs).

Table 3. The Features of Different Classes

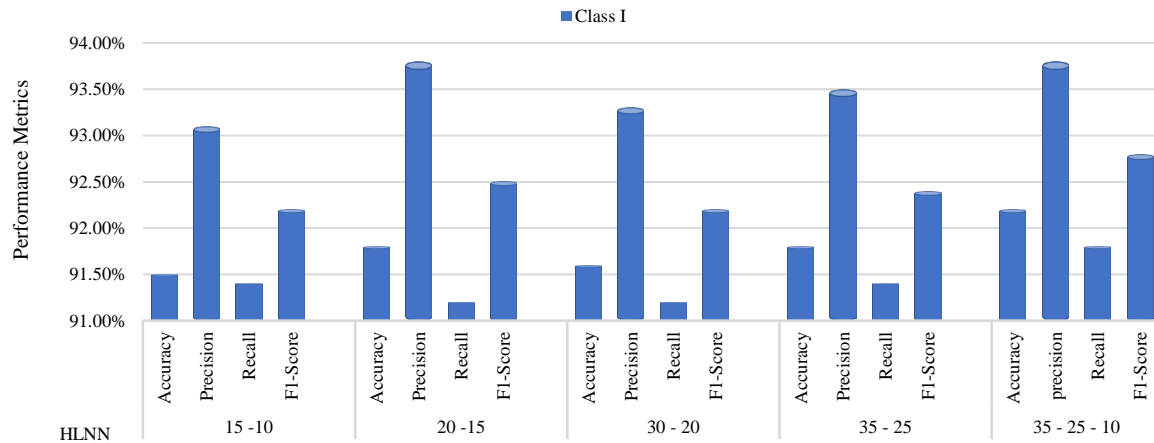| Classes | Features |
|---------|----------|
| Class I | F1 |
| Class II | F1, F2 |
| Class III | F1, F2, F3 |
| Class IV | F1, F2, F3, F4 |
| Class V | F1, F2, F3, F4, F5 |
| Class VI | F1, F2, F3, F4, F5, F6 |



Fig. 9. The performance at class I

To overcome this issue, new features are proposed to increase the reliability and dependability of the proposed method in conjunction with (F1). One such feature is the average odd harmonic (F2), which prevents false trips during load switching at low loading ratios. However, this feature cannot solve all the issues in switching events at high load switching. The average even harmonic (F3) is an influential feature added to increase the security of the proposed method and prevent false tripping during non-fault events, especially at inrush current and capacitor bank switching events. The effectiveness of this feature can be observed in Fig. 10, where it is demonstrated that the detection performance is improved compared to the results in Class I. Another feature, F4, is proposed to address problems during switching events at low and heavy loading switches and solve some problems caused by non-linear load switching. The inclusion of this feature is particularly promising, as it contributes to increasing the accuracy and dependability of the proposed method. By utilizing this feature in combination with the previous ones, the overall results show a significant improvement in the classification of HIF from other non-fault events, as shown in the results at class IV and that depicted in Fig. 11. The presence of non-linear loads poses a significant challenge to detecting HIF, as the features of HIF and NLLs are often quite similar. Inter-harmonic energy (F5) has been proposed to address this issue as a valuable addition to the previously proposed features. Using this feature, in combination with the features of F1 and F4, significantly enhances the proposed method's ability to distinguish between HIF and NLLs, as shown in the result of Class V depicted in Fig. 11. Lastly, the PSD has been proposed to support the previously proposed features, particularly in cases of inrush current, capacitor bank switching, and some cases of load switching. The inclusion of PSD improves the overall accuracy and dependability of the proposed method and allows for better classification and differentiation of HIF from other non-fault events. Fig. 12 and Fig. 13 show the effectiveness of adding these features to improve the overall detection accuracy compared with the results of the previous classes, where the accuracy of 99.3% at an HLNN structure of 35-25, with an associated mean squared error (MSE) of 0.0108.
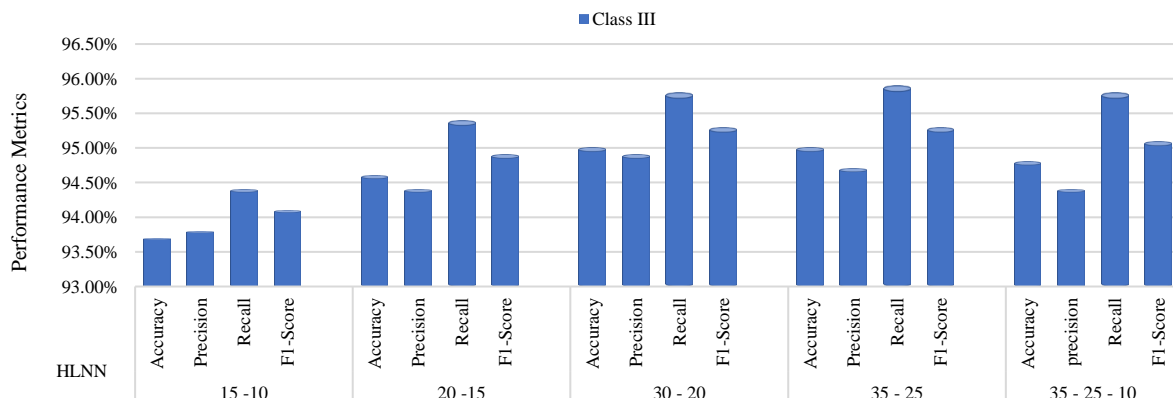


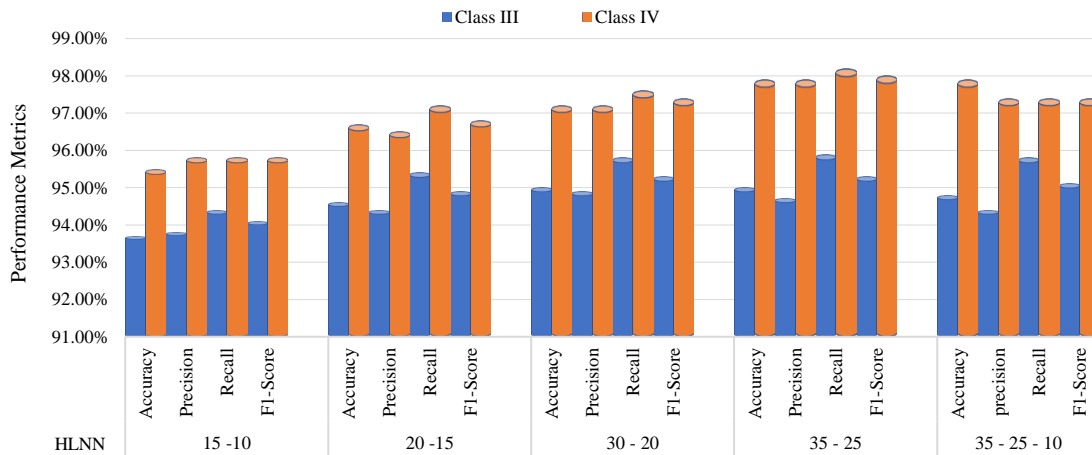Fig. 10. The performance at the class III

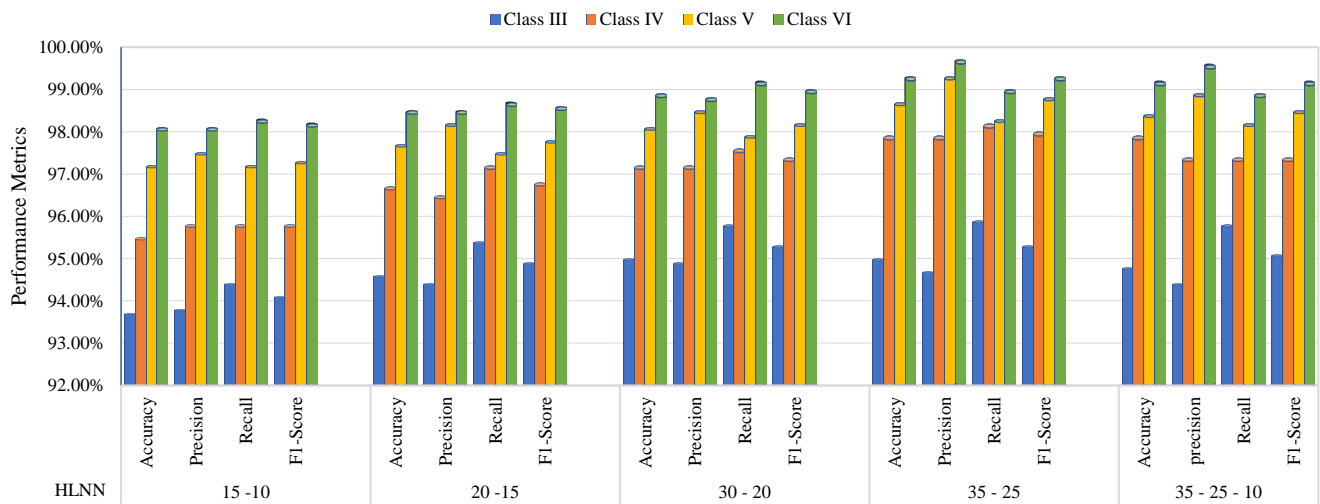Fig. 11. The performance comparison of class III and class IV



Fig. 12. The performance comparison of class III, class IV, class V, class VI
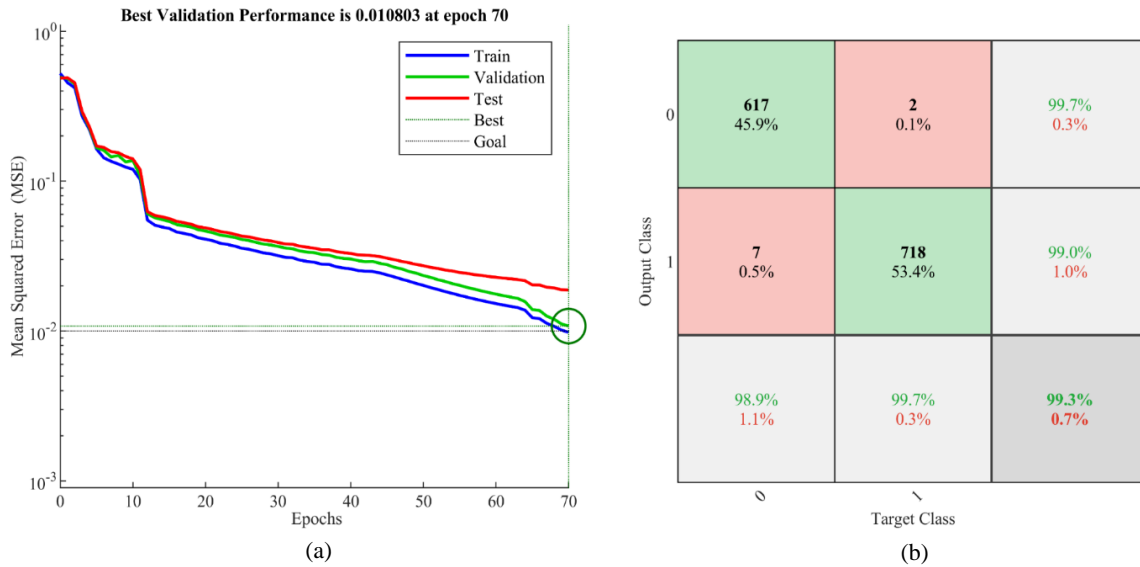


Fig. 13. a) MSE Performance, b) Confusion matrix

It should be noted that the results presented were obtained through a comprehensive analysis of each feature utilized in this study. Based on the output generated by the ANN tool during the classification process, we have arrived at these conclusions regarding the impact of the proposed features on event classification performance.

For comparison purposes with related studies, the authors in [2] proposed an approach that combines third and even-order harmonics based on the non-linearity and asymmetry properties during high impedance faults (HIF) and switching events. Concurrently, the authors in [32] introduced a method based on the inter-harmonic content in the current signal, which is associated with the randomness variations of HIF. However, the authors in [2] did not consider the presence of nonlinear loads in the test scenario, and the authors in [32] overlooked the inclusion of switching events in the test scenario. These oversights render both methods vulnerable, affecting their overall performance. The proposed detection method in this study incorporates low-order harmonics and inter-harmonic content, as well as the PSD of the current signal during HIF and non-HIF events, including linear and nonlinear load switching, capacitor bank switching, and transformer energization. This combination of features addresses the classification challenges of distinguishing HIF from other healthy events and enhances the performance of the proposed method under various operating conditions.

In conclusion, combining all features proposed in the methodology provided excellent detection rates for HIF. It was observed that these features significantly overlapped in some events, making it challenging to separate them using conventional methods based on threshold values. To overcome this obstacle, a Back-propagation Neural Network (BPNN) was used in this study to classify these features and identify HIF. It should be mentioned that the harmonics present in the distribution network were not considered because a comprehensive study of the harmonic behavior in the distribution networks is required to assess the proposed approach and suggest appropriate solutions to designing an effective practical technique.

## 6. Conclusion

This paper proposes a method for detecting HIF in distribution feeders. The method employs a combination of FFT and ANNs techniques to analyze signals and determine the occurrence of HIF. FFT is utilized to extract low-order frequency spectrum (FS) magnitudes, which are then used to calculate the proposed features. The study includes six classes, and each class is characterized by a set of features that were entirely tested in this paper. The simulation was conducted on a radial overhead distribution feeder using MATLAB/Simulink under various conditions and rigorous test scenarios, including the existence of non-linear loads, different fault locations, various inception angles, and different HIF surfaces. The results indicated that the combination of even and odd low-order harmonics and the second and third-order harmonics feature is insufficient to obtain high HIF detection accuracy, especially in the presence of non-linear loads. However, the addition of inter-harmonic energy and PSD features to these existing features has significantly improved the detection and distinction of HIFs from other non-HIF events, such as inrush current, linear and non-linear load switching, and capacitor bank switching, with an accuracy of 99.3%, irrespective of HIF location and resistance. The robustness of the classifier was also evaluated using accuracy, recall, precision, and F1-score. The results show that the ANN techniques have demonstrated excellent performance in accurately detecting and classifying HIFs from other non-HIF events in the distribution system.

## Acknowledgment

## References

[1]  Tengdin, John, Ron Westfall, and Kevin Stephan."High Impedance Fault Detection Technology," in "Report of PSRC Working Group D15," Mar. 1996, Available: https://grouper.ieee.org/groups/td/dist/documents/highz.pdf.

[2]  A. Soheili, J. Sadeh, H. Lomei, and K. Muttaqi, "A new high impedance fault detection scheme: Fourier based approach," in 2016 IEEE International Conference on Power System Technology (POWERCON), 2016, pp. 1-6. doi: https://doi.org/10.1109/POWERCON.2016.7754052.

[3]  S. Chakraborty and S. Das, "Application of Smart Meters in High Impedance Fault Detection on Distribution Systems," IEEE Transactions on Smart Grid, vol. 10, no. 3, pp. 3465-3473, 2019. doi: https://doi.org/10.1109/TSG.2018.2828414.

[4]  H. Bai, B. Tang, T. Cheng, and H. Liu, "High impedance fault detection method in distribution network based on improved Emanuel model and DenseNet," Energy Reports, vol. 8, pp. 982-987, Nov 2022. doi: https://doi.org/10.1016/j.egyr.2022.05.199.

[5]  A. Aljohani and I. Habiballah, "High-Impedance Fault Diagnosis: A Review," vol. 13, no. 23, p. 6447, 2020. doi: https://doi.org/10.3390/en13236447.

[6]  B. Hao, "AI in arcing-HIF detection: a brief review," vol. 3, no. 4, pp. 435-444, 2020. doi: https://doi.org/10.1049/iet-stg.2019.0091.

[7]  S. Khavari, R. Dashti, H. R. Shaker, and A. Santos, "High Impedance Fault Detection and Location in Combined Overhead Line and Underground Cable Distribution Networks Equipped with Data Loggers," vol. 13, no. 9, p. 2331, 2020. doi: https://doi.org/10.3390/en13092331.

[8]  S. Wang and P. Dehghanian, "On the Use of Artificial Intelligence for High Impedance Fault Detection and Electrical Safety," IEEE Transactions on Industry Applications, vol. 56, no. 6, pp. 7208-7216, 2020. doi: https://doi.org/10.1109/TIA.2020.3017698.

[9]  P. Obi, E. Amako, and C. Ezeonye, "High impedance fault arc analysis on 11 kV distribution networks," Nigerian Journal of Technological Development, vol. 19, no. 2, pp. 143-149, 2022. doi: https://doi.org/10.4314/njtd.v19i2.6.

[10] D. A. Gadanayak and R. K. Mallick, "Interharmonics based high impedance fault detection in distribution systems using maximum overlap wavelet packet transform and a modified empirical mode decomposition," International Journal of Electrical Power & Energy Systems, vol. 112, pp. 282-293, Nov 2019. doi: https://doi.org/10.1016/j.ijepes.2019.04.050.

[11] A. Soheili, J. Sadeh, and R. Bakhshi, "Modified FFT based high impedance fault detection technique considering distribution non-linear loads: Simulation and experimental data analysis," International Journal of Electrical Power & Energy Systems, vol. 94, pp. 124-140, Jan 2018. doi: https://doi.org/10.1016/j.ijepes.2017.06.035.

[12] K. Sekar, N. K. Mohanty, and A. K. Sahoo, "High impedance fault detection using wavelet transform," in Technologies for Smart-City Energy Security and Power (ICSESP), 2018, pp. 1-6. doi: https://doi.org/10.1109/ICSESP.2018.8376740.

[13] B. K. Chaitanya, A. Yadav, and M. Pazoki, "High Impedance Fault Detection Scheme for Active Distribution Network Using Empirical Wavelet Transform and Support Vector Machine," in 15th International Conference on Protection and Automation of Power Systems (IPAPS), 2020, pp. 149-152. doi: https://doi.org/10.1109/IPAPS52181.2020.9375620.

[14] S. Silva, P. Costa, M. Gouvea, A. Lacerda, F. Alves, and D. Leite, "High impedance fault detection in power distribution systems using wavelet transform and evolving neural network," Electric Power Systems Research, vol. 154, pp. 474-483, Jan 2018. doi: https://doi.org/10.1016/j.epsr.2017.08.039.

[15] T. Sirojan, S. Lu, B. T. Phung, D. Zhang, and E. Ambikairajah, "Sustainable Deep Learning at Grid Edge for Real-Time High Impedance Fault Detection," IEEE Transactions on Sustainable Computing, vol. 7, no. 2, pp. 346-357, 2022. doi: https://doi.org/10.1109/TSUSC.2018.2879960.

[16] É. M. Lima, N. S. D. Brito, and B. A. d. Souza, "High impedance fault detection based on Stockwell transform and third harmonic current phase angle," Electric Power Systems Research, vol. 175, p. 105931, Oct 2019. doi: https://doi.org/10.1016/j.epsr.2019.105931.

[17] D. Guillen, J. Olveres, V. Torres-García, and B. Escalante-Ramírez, "Hermite Transform Based Algorithm for Detection and Classification of High Impedance Faults," IEEE Access, vol. 10, pp. 79962-79973, 2022. doi: https://doi.org/10.1109/ACCESS.2022.3194525.

[18] H. Lala and S. Karmakar, "Detection and Experimental Validation of High Impedance Arc Fault in Distribution System Using Empirical Mode Decomposition," IEEE Systems Journal, vol. 14, no. 3, pp. 3494-3505, 2020. doi: https://doi.org/10.1109/JSYST.2020.2969966.

[19] K. Moloi and I. Davidson, "High Impedance Fault Detection Protection Scheme for Power Distribution Systems," vol. 10, no. 22, p. 4298, 2022. doi: https://doi.org/10.3390/math10224298.

[20] H. Shu, Y. Deng, J. Dong, P. Cao, B. Yang, and Z. Bo, "A detection method of high impedance arcing fault for distribution network with distributed generation based on CEEMDAN and TEO algorithm," vol. 31, no. 8, p. e12926, 2021. doi: https://doi.org/10.1002/2050-7038.12926.

[21] O. A. Gashteroodkhani, M. Majidi, and M. Etezadi-Amoli, "Fire hazard mitigation in distribution systems through high impedance fault detection," Electric Power Systems Research, vol. 192, p. 106928, Mar 2021. doi: https://doi.org/10.1016/j.epsr.2020.106928.

[22] K. Rai, F. Hojatpanah, F. B. Ajaei, J. M. Guerrero, and K. Grolinger, "Deep learning for high-impedance fault detection and classification: transformer-CNN," Neural Computing and Applications, vol. 34, no. 16, pp. 14067-14084, Aug 2022. doi: https://doi.org/10.1007/s00521-022-07219-z.

[23] H. G. Yeh, S. Sim, R. Yinger, and R. Bravo, "A comparative study of orthogonal algorithms for detecting the HIF in MDCs," in 2017 IEEE Green Energy and Smart Systems Conference (IGESSC), 2017, pp. 1-7. doi: https://doi.org/10.1109/IGESC.2017.8283456.

[24] V. C. Nikolaidis, A. D. Patsidis, and A. M. Tsimtsios, "High impedance fault modelling and application of detection techniques with EMTP-RV," vol. 2018, no. 15, pp. 1120-1124, 2018. doi: https://doi.org/10.1049/joe.2018.0217.

[25] S. Roy and S. Debnath, "PSD based high impedance fault detection and classification in distribution system," Measurement, vol. 169, p. 108366, Feb 2021. doi: https://doi.org/10.1016/j.measurement.2020.108366.

[26] M. S. Hassan, K. Kamal, and T. A. H. Ratlamwala, "Fault classification of power plants using artificial neural network," Energy Sources, Part A: Recovery, Utilization, and Environmental Effects, vol. 44, no. 3, pp. 7665-7680, Sep 2022. doi: https://doi.org/10.1080/15567036.2022.2113936.

[27] N. B. Roy and K. Bhattacharya, Application of Signal Processing Tools and Artificial Neural Network in Diagnosis of Power System Faults. CRC Press, 2021.

[28] M. Mishra and R. R. Panigrahi, "Taxonomy of high impedance fault detection algorithm," Measurement, vol. 148, p. 106955, Dec 2019. doi: https://doi.org/10.1016/j.measurement.2019.106955.

[29] K. Rai, F. Hojatpanah, F. Badrkhani Ajaei, and K. Grolinger, "Deep Learning for High-Impedance Fault Detection: Convolutional Autoencoders," vol. 14, no. 12, p. 3623, 2021. doi: https://doi.org/10.3390/en14123623.

[30] P. Rai, N. D. Londhe, and R. Raj, "Fault classification in power system distribution network integrated with distributed generators using CNN," Electric Power Systems Research, vol. 192, p. 106914, Mar 2021. doi: https://doi.org/10.1016/j.epsr.2020.106914.

[31] K. S. V. Swarna, A. Vinayagam, M. Belsam Jeba Ananth, P. Venkatesh Kumar, V. Veerasamy, and P. Radhakrishnan, "A KNN based random subspace ensemble classifier for detection and discrimination of high impedance fault in PV integrated power network," Measurement, vol. 187, p. 110333, Jan 2022. doi: https://doi.org/10.1016/j.measurement.2021.110333.

[32] J. R. Macedo, J. W. Resende, C. A. Bissochi Jr, D. Carvalho, and F. C. Castro, "Proposition of an interharmonic-based methodology for high-impedance fault detection in distribution systems," vol. 9, no. 16, pp. 2593-2601, 2015. doi: https://doi.org/10.1049/iet-gtd.2015.0407.